Urea and guanidinium induced denaturation of a Trp-cage miniprotein

Jan Heyda,[1] Milan Kožíšek,[1] Lucie Bednárova,[1] Gary Thompson,[2] Jan Konvalinka,[1] Jiří Vondrášek,[1] and Pavel Jungwirth[1*]

[1]*Institute of Organic Chemistry and Biochemistry, Academy of Sciences of the Czech Republic, and Center for Biomolecules and Complex Molecular Systems, Flemingovo nám. 2, 16610 Prague 6, Czech Republic*

[2]*Astbury Centre for Structural Molecular Biology, Faculty of Biological Sciences, University of Leeds, Leeds LS2 9JT, U.K.*

*Corresponding author: e-mail pavel.jungwirth@uochb.cas.cz

Abstract

Using a combination of experimental techniques (circular dichroism, differential scanning calorimetry, and NMR) and molecular dynamics simulations we performed an extensive study of denaturation of the Trp-cage miniprotein by urea and guanidinium. The experiments, despite their different sensitivities to various aspects of the denaturation process, consistently point to simple, two-state unfolding process. Microsecond molecular dynamics simulations with a femtosecond time resolution allow to unravel the detailed molecular mechanism of Trp-cage unfolding. The process starts with a destabilizing proline shift in the hydrophobic core of the miniprotein, followed by a gradual destruction of the hydrophobic loop and the α-helix. Despite differences in interactions of urea vs guanidinium with various peptide moieties, the overall destabilizing action of these two denaturants on Trp-cage is very similar.

Introduction

Significant effort has been dedicated to elucidating the molecular mechanisms of the effect of chemical denaturants on protein stability. For the two most common denaturants, urea and guanidine hydrochloride, direct interactions with the protein backbone and side chains, as well as indirect effects due to interaction with water molecules were investigated recently.[1-6] Guanidinium was shown to act preferentially on charged residues and, due to the charge delocalization, it also has tendency to stack with aromatic side chains of Trp, Phe, Tyr and His in the protein interior and thus significantly contributes to protein unfolding .[6,7] Urea, in addition to the binding of charged and polar residues significantly influences polar interactions within the protein backbone by binding to carbonyl oxygen and contributes to destabilization of secondary structure elements.[7-9]

In order to assess the details and specificity of the denaturant-protein interactions it is useful to employ a small but realistic model protein system. In this context, the Trp-cage miniprotein has become the ”hydrogen atom” of the protein folding/unfolding field recently.[10] First synthesized in 2002 as a C-terminal fragment of exendin-4, it is the shortest known self-folding peptide.[11] With only 20 amino acids (NLYIQWLKDGGPSSGRPPPS) it already possesses a well developed α–helix, a short meander, and a hydrophobic loop in-between, which all form spontaneously and fold into a simple tertiary structure within 4 μs.[12,13] Therefore, the fast folding and unfolding of this miniprotein with structural features present also in larger proteins is within the reach of atomistic molecular dynamics (MD) simulations. One has to bear in mind, however, that due to its limited size Trp-cage represents a system where an important

secondary structure motif – a β-sheet is absent, not to mention more complex tertiary and quaternary structures, which can be involved during folding and unfolding dynamics of more complex proteins.

A lot can be learned already from the "hydrogen atom" of protein folding, which is reflected in the large number of experimental[11-21] and computational[3,22-35] studies dedicated to the structural and dynamical properties of Trp-cage and its mutants. NMR has been used to determine the structure of Trp-cage, while circular dichroism (CD) and differential scanning microcalorimetry (DSC) have been employed to elucidate the dynamics and thermodynamics of the folding/unfolding process.[11-14] A simulation technique, that has been widely used for investigations of folding/unfolding of Trp-cage is the Replica Exchange Molecular Dynamics (REMD).[26,28-30,36-38] REMD allows for efficient sampling of the configuration space of the peptide by swapping between MD runs at different temperatures. The first studies of Trp-cage using this technique, albeit with a submicrosecond total simulation time, suggested a two state folding process[26] or two pathways folding mechanism[28,38]. Later REMD studies employed total simulation times comparable to or larger than the experimental folding time,[29,30] which allowed for converged sampling of the configurational space. Due to deficiencies in force field , these simulations, however, yielded, an unrealistically high unfolding temperature of about 440 K,[29,30] compared to the experimental value of 315 K.[27]

Only with improved interaction potentials was the correct unfolding temperature achieved.[39] With extensive configurational sampling (total simulation time of 100 μs) these calculations allowed for determining the conditions for both warm and cold denaturation

processes, as well as for pressure denaturation.[39] Aside from temperature, another denaturation agent which has been scrutinized by REMD and experiment is urea.[3] In accord with the general notion of urea as a denaturating agent simulations show that it shifts the equilibrium between folded and unfolded Trp-cage geometries toward the latter, reducing thus effectively the denaturation temperature. This change in denaturating temperature is proportional to concentration and several moles per liter of urea are necessary for an appreciable effect.[3]

The effect of guanidine hydrochloride, as another common denaturating agent, on Trp-cage has not been investigated computationally yet, with only a single fluorescence correlation spectroscopy study touching upon this issue.[40] The common wisdom has been that positively charged guanidinium acts like urea plus the corresponding amount of neutral salt such as NaCl.[41] This may, however, be an oversimplification since a detailed comparison between urea and guanidinium reveals that they interact with proteins in a different way.[8] As mentioned above, urea tends in particular to replace water molecules next to the backbone (most likely due to preferential dispersion interaction),[3] while guandinium is quite "promiscuous" in that it preferentially interacts with both hydrophobic (primarily aromatic) and charged groups, including arginine, which is also positively charged.[6,42,43] In this study we compare the effects of urea and guanidinium on Trp-cage denaturation. DSC, CD, and NMR techniques were used to characterize the native and denatured species, together with extensive direct MD simulations aimed at elucidating the unfolding pathways of Trp-cage in the presence of urea and guanidinium. MD simulations and the three experimental techniques provide a complementary

and consistent picture of Trp-cage denaturation, with the former focusing on the unfolding dynamics and the latter on characterizing the miniprotein before and after denaturation.

Materials and Methods

Trp-cage peptide (structure 1L2Y in the Protein Data Bank) was purchased from AnaSpec Inc. (Fremont, CA, USA; cat.#62072). Guanidine hydrochloride and urea were ordered from Sigma (St. Louis, MO, USA; cat.#G4505 and U5378) unless stated otherwise.

Circular dichroism spectroscopy

CD measurements were performed on a Jasco-815 spectropolarimeter. The spectra were measured from 190 nm to 260 nm (with a scanning speed of 20nm/min, response time of 4 s, and pairs spectra acquired to validate repeatability) in a 1mm quartz cell. The Trp-cage concentration was kept constant at 0.1mg/ml. The spectra were measured in 0 – 4 M of urea and 0 - 2.5 M of guanidine hydrochloride, in each case with 20 mM of sodium phosphate buffer (PBS) to maintain pH = 7.0. The temperature of the sample was kept constant at 2 °C using a Peltier type temperature control system PTC-423S/L.

Temperature dependent elipticity measurements were performed in a 1cm quartz cell which was stirred. The Trp-cage concentration was 0.01mg/ml , with 20 mM sodium phosphate buffer and with added 1 or 2 M of urea or 0.5 or 1 M of guanidine hydrochloride. Measurements were performed in the temperature interval of 2 - 95 ^{O}C with an increment of 2 °C, temperature gradient of 25 °C per hour, and response time of 32 s. The ellipticity at 222

nm as indicator of a α-helical structure was monitored, with circular polarization expressed as molar elipticity per residue. Assuming the two-state model the observed mean residue elipticity at 222 nm could be converted into α-helical fraction (f_H).[44] Reversibility of folding in all these systems was examined by measuring the CD spectrum at 2 °C after unfolding at high temperature and it was found to be high (about 85%) only in the solution without denaturants.

Differential scanning calorimetry

Thermal denaturation experiments of the Trp-cage miniprotein in the presence of guanidine hydrochloride (GdmCl) or urea at varying concentrations were performed on a high precision VP-DSC differential scanning calorimeter (MicroCal, GE Healthcare, Northampton, MA, USA). Trp-cage miniprotein was dissolved in 20mM sodium phosphate (pH 7.0) or in the same buffer containing urea or GdmCl to final peptide concentration of 345μM (0.75mg/ml). The exact peptide concentration was determined by the HPLC amino acid analysis. The peptide sample and the buffer reference solution were degassed by stirring under vacuum and carefully loaded into the calorimeter cells in order to avoid bubble formation. The solutions were heated from 10 to 120 °C at a rate of 1 °C/min. The denaturation profiles were superimposed after baseline correction using the MicroCal Origin software. The reversibility of heat denaturations was monitored by repeating the experiment with already heated samples cooled back to 10°C, with the second scan performed after 15 min of thermostating.

NMR spectroscopy

NMR spectra were measured on a Varian Inova spectrometers at a field strength of 500MHz using a room temperature ^{1}H ^{13}C ^{15}N triple resonance probe with Z axis pulsed field gradients. Each sample contained 1mg of Trp-cage giving a final concentration of 1.53mM in 300μL of an aqueous buffer containing 15mM sodium phosphate at a pH or pH* of 7.0 for D_2O or H_2O samples respectively. ^{1}H-^{1}H NOESY and TOCSY assignment spectra were measured in a 10%D_2O:90%H_2O solution and all ^{1}H-^{13}C HSQC spectra were measured in 99% D_2O. Urea (MP Biomedicals ultra pure) and guanidine hydrochloride (Melford > 99%) stocks were repeatedly dissolved in 99% D2O (Goss) and lyophilised (urea) or rotary evaporated (guanidine hydrochloride) three times to give deuteration levels > 99%. All NMR spectra were acquired at 280K. ^{1}H-^{1}H NOESY and TOCSY spectra with watergate water suppression[45] were recorded with mixing times of 150ms and 70s respectively, and sweep widths of 6712 Hz with 1024 and 256 points collected in F2 and F1 and using 40 transients per FID. Natural abundance ^{1}H- ^{13}C HSQC spectra were measured with a sweep widths of 8525Hz and 10000Hz in the ^{1}H and ^{13}C dimension, using 316 transients and acquiring 1024 points and 80 increments in the direct and indirect dimensions with a sensitivity enhanced sequence.[46] Both ^{1}H and ^{13}C chemical shifts were directly referenced to the methyl groups in 4,4-dimethyl-4-silapentane-1-sulfonic acid (DSS). Denaturant concentrations were measured using a Ceti 8200 reftractometer using the equations described by Pace et al.[47] NMR data were processed using nmrpipe[48] and analyzed in CCPN Analysis.[49] Data extraction and correlation plots were carried out using custom python scripts and PyLab (http://matplotlib.sourceforge.net). Analysis of titration curves using non negative matrix factorizations was carried out using the ChemoSpec

(http://github.com/bryanhanson/ ChemoSpec.git) and NMFN (http://cran.r-project/web/packages/NMFN/index.html) packages.

Molecular dynamics simulations

MD simulations were performed to study the behavior of Trp-cage miniprotein (PDB code 1L2Y) in different denaturing environments at ambient temperature. The aspartic acid, arginine, and lysine residues were charged, in accord with their protonation state at neutral pH. The N terminus of Trp-cage was acetylated and its C terminus was alkylated. All simulations started from the experimental NMR structure and were performed using the Amber 10 program.[50] Three simulations were performed. In the first simulation, referred to as the neat water simulation, the Trp-cage molecule was surrounded by 1433 water molecules and one chloride anion was added to compensate the total charge of the miniprotein. In the second simulation, Trp-cage was simulated with 1309 water molecules and 48 urea molecules (forming a 2M urea solution). In the third simulation, 1262 water molecules, 48 guanidinium cations, and 49 chloride anions (forming a 2M guanidinium solution) were added to Trp-cage. In all simulations the SPC/E water model[51] together with parameters for the chloride anion,[52] and guanidinium cation[53] were employed. For urea, the Lennard-Jones parameters for N, H, and C were the same as those for guanidinium, and those for the carbonyl O were taken from parm99.[54] Partial charges were evaluated using the RESP procedure at the HF/6-31g* level, as recommended for the Amber force field.[55] For comparison, we also ran test Trp-cage

denaturing simulations with the Kirkwood-Buff parameterization of urea,[56] which gave qualitatively similar results. For the Trp-cage the parm99 parameters were used.[54]

Before the production runs each of the systems was energy minimized, heated up to 300 K in 1 ns, pressurized to 1 atm within 1ns, and further equilibrated for another 1 ns, with a 1fs time step employed. This procedure ensured that the environment around Trp-cage homogenized sufficiently, and the Trp-cage structure itself was not perturbed during the heating phase. The pre-equilibrated system was used for production MD simulations. The total simulation time was 1 μs per trajectory, with coordinates saved every 1 ps, yielding 1 000 000 frames for further analysis. The equilibrated box size was approximately 36 × 36 × 36 Å. 3D periodic boundary conditions were applied with long-range electrostatic interactions beyond the non-bonded cutoff of 8 Å accounted for using the particle mesh Ewald (PME) method.[57] The Berendsen temperature (300 K) and pressure (1 atm) couplings were employed,[58] and all bonds containing hydrogens were constrained using the SHAKE algorithm.[59]

Results and Discussion

Circular dichroism spectroscopy

Analysis of the CD spectra was performed according to a procedure presented in Ref. [60]. Ellipticity at 222 nm, Θ_{222}, is assumed to be linearly related to mean helix content, f_H, which can be calculated from the Lifson-Roig-based helix-coil model (see below). The conversion of Θ_{222} to f_H requires the knowledge of the baseline ellipticities of both the random coil, Θ_c and the complete helix, Θ_H The values of Θ_c and Θ_H are dependent on temperature and are given by the following expressions:

$f_H = (\Theta_{222} - \Theta_c)/ (\Theta_H - \Theta_c)$ (1)

The values of Θ_C and Θ_H are dependent on temperature andare given by the following expressions:

$\Theta_c = 2220 - 53T$ (2)

and

$\Theta_H = (-44\ 000 + 250T)(1 - 3/N_r)$ (3)

where T is the temperature in °C and N_r is the chain length in residues. For our calculation Θ_c= 3900 and Θ_H=38000.

CD spectra of Trp-cage were first measured under the previously reported experimental conditions without denaturating agents and the thermal unfolding of Trp-cage was compared to the literature data.[14] The CD spectrum (fig. 1) as well as the curve of thermal unfolding (fig. 2) were in good agreement with previous results and the assumption of the two-state folding mechanism was thus further supported.[14] In neat water at the experimental temperature of 2 °C the miniprotein is practically completely folded.[11] Our spectra confirm that under these conditions Trp-cage contains a well developed α-helix. Assuming that the miniprotein contains only α-helical and disordered parts, the α-helical fraction f_H[61] was calculated as f_H (at 2 °C, in PBS) = 46%.

Thermal unfolding of Trp-cage in the presence of denaturating agents (urea or GdmCl) at varying concentrations was then measured (fig. 3 and figs. S1 and S2 in the Supplemetray Information), with the results also expressed in terms of α-helical fraction f_H. The results obtained in the presence of urea (1 and 2 M) were in a very good agreement with the literature.[62] The α-helical fraction of Trp-cage decreased from the value of 46% in water (f_H (at

2 °C, in PBS) = 46%), to 41% in 1 M urea and 37% in 2 M urea. When temperature was increased to 95^{O}C the α-helical fraction in all the samples decreased below 20%. Adding GdmCl (0.5 and 1 M) to Trp-cage also caused unfolding of the peptide. Adding 0.5 M of GdmCl at 2 °C lead to a decrease of the portion of α-helical fraction to 40%, which is equivalent to the effect of 1M of urea. A similar effect was observed when 1M GdmCl was added to the peptide solution yielding an α-helical fraction about 32%. Futher addition of either GdmCl or urea resulted in a gradual decrease of the α-helical fraction f_H below 20%, which corresponded to the α-helical fraction f_H reached by the thermal unfolding.

Differential scanning calorimetry

To investigate the effects of GdmCl and urea on the thermal unfolding of Trp-cage miniprotein, denaturation experiments were performed using a differential scanning calorimeter. Trp-cage at a concentration of 0.75mg/ml was heated alone and in the presence of the denaturants at a rate of 1°C/min from 10 to 120 °C. Cooling and additional rescannings of the peptide samples showed that the thermal unfoldings of Trp-cage were irreversible. DSC thus allowed us to determine the trends of the thermal unfolding rather than the thermodynamic values such as heat capacity change or calorimetric transition enthalpy. Denaturations in the presence of guanidine hydrochloride showed that GdmCl even at a very low concentration of 0.05 M has a significant effect on peptide denaturation (fig. 4). The transition temperature further decreased with the increase of GdmCl concentration as expected, and the heat capacity change was significantly reduced. Unlike in CD spectroscopy, a very significant effect on heat capacity was observed even in the lowest GdmCl concentrations

used. It is difficult to speculate about the possible explanation for this observation at this stage, but possibly the higher temperature at which large changes in DSC curves are observed provides some clue (indeed at the temperature of 2 ^{o}C of the CD experiment presented in fig. 3 there is little difference between the DSC curves with varying guanidinium concentrations).

Unexpected thermal denaturation curves were obtained when Trp-cage was heated in the presence of urea (compare fig. S3 in Supproting Information). An exothermic denaturation peak was observed when the sample was heated. The gel chromatography analysis of the processed sample showed monodisperse peptide of expected molecular size in the solution, suggesting that the observed exothermic peak is not caused by potential multimerization of the peptide in solution (data not shown). We also observed an increase in the pH of solution after heating, probably due to the release of ammonia. Finally, mass spectrometry analysis revealed covalent modification of the peptide by up to two urea molecules during heat denaturation of Trp-cage peptide (data not shown) that can explain the exothermic peak observed by DSC. A similar modification of proteins upon heating has already been observed upon heating of ribonuclease or hemoglobin in slightly acidic conditions, which promoted the reaction of cysteine sulfhydryls or ε-aminogroups of lysines with residual cyanate derived from urea, leading to protein carbamylation.[63,64] The exact chemistry of peptide modification by urea in the case of Trp-cage peptide will be further analysed and published elsewhere.

Due to the covalent modification of analysed peptide by denaturant, no direct conclusions about the thermodynamics of Trp-cage peptide denaturation by urea could be drawn from the DSC experiments. Potential covalent modifications of proteins by urea must be

considered in all experiments involving heating in protein solutions in the presence of urea. Interestingly, this effect seems to be protein specific: no covalent modification of lysozyme by urea was observed, either in our laboratory (data not shown) or in the literature.[65]

NMR spectroscopy

NMR experiments were carried out to ascertain if intermediate species, other than the unfolded and folded state could be detected on a per residue basis during the unfolding of Trp-cage using urea and guanidine hydrochloride. The folded state ^{1}H-^{13}C HSQC spectrum of Trp-cage (fig. 5) was assigned based on the previous assignments described by Neidigh et al.[11] (BMRB code 5292) using ^{1}H-^{1}H TOCSY and NOESY spectra measured with Trp-cage dissolved in 90%H_2O:10%D_2O. Unfolding was then carried out using urea and guanidinium (pH 7.0, 15 mM sodium phosphate, and 280 K) with titration points at 0, 1, 2, 3, 4 and 5 M for urea and 0, 0.33, 0.65, 1.5, and 2.7 M for guanidinium. Fig. 6 shows representative examples of titrations of peaks from Hα–Cα of residues Tyr-3, Pro-12 and Pro-19 (note no peak was detected for the Hα–Cα peak of residues 18 and 11 and data from the glycine Hα2 and Hα3 peaks were not used as they overlapped too strongly at high denaturant concentrations). The peaks of the unfolded and intermediate states were identified by following the movement of Hα-Cα peaks throughout the spectrum as the titration proceeded since as expected all the species present were in fast exchange as indicated by the lack of any extra peaks appearing during the course of the titration for both urea and guanidinium (fig. 7 shows the unfolded spectrum of Trp-cage in urea).

As the observed unfolding curve did not have a clear folded state plateau a series of three increasingly more sophisticated methodologies were used to determine if more that one species was present or if particular residues showed changes in Hα-Cα chemical shift which were not correlated with those from the rest of the residues in the protein. At the simplest level of analysis if during a titration a native species N converts to unfolded species U. U and N are in fast exchange on the chemical shift timescale and have concentrations [U] and [N]. The observed chemical shift Ω_o will change from Ω_U and Ω_N with intermediate chemical shifts being given by the shifts of Ω_U and Ω_N weighted by the concentrations U and N (eq. 1) resulting in a linear change in chemical shifts.

$$\Omega_o = [U]\Omega_U + [N]\Omega_N \quad (4)$$

If an intermediate species I is present during the titration with the reaction being N $\rightleftharpoons$ I $\rightleftharpoons$ U and where the chemical shifts are not equal (i.e. $\Omega_I \neq \Omega_N$ and $\Omega_I \neq \Omega_U$) the observed chemical shifts will again change smoothly from Ω_N to Ω_U. However, since the intermediate chemical shifts between Ω_U and Ω_N will be a weighted combination of the shifts of U, I and N ($\Omega_U, \Omega_I, \Omega_N$; eq. 2)

$$\Omega_o = [U]\Omega_U + [I]\Omega_I + [N]\Omega_N \quad (5)$$

and the term $[I]\Omega_I$ is not present in the initial or final shifts, if the combination of [I] and Ω_I are large enough a deviation from the linear behavior expected in equation 4 will be observed. Therefore the ^{1}H and ^{13}C chemical shifts for each residue were fitted to each other over the range of denaturant concentrations used using a linear least squares fit and the value of the

correlation coefficient R used to analyze for deviations from linearity. Little deviation was observed (typical R > 0.99) except in the case of residues with small chemical shift ranges in one of the chemical shift dimensions or where overlap was a major factor.

Since ^{1}H and ^{13}C shifts are expected to be partially correlated as they share similar chemical shift environments, and because ^{1}H chemical shifts can be more accurately measured due to the higher digital resolution available in the direct dimension of ^{1}H - ^{13}C HSQC spectra, as a further more sensitive test all ^{1}H chemical shifts for all pairs of residues were correlated and a linear fit applied for each denaturant. In this analysis distinct deviations for the first and last residue in Trp-cage were observed and attributed to 'end effects' . Performing the same analysis without chemical shifts from Hα1 and Hα20 resulted in correlations from 0.982±0.008 (residue 19) to 0.995±0.008 (residue 2) for urea and 0.989±0.008 (residue 8) and 0.963±0.022 (residue 5) for guanadinium (fig. 6).

Non negative matrix factorization (nnmf)[66] was used as the most sensitive method to assess whether there were small amounts of another species present. Nnmf is described by equation 6

$$\text{nnmf}(X) \rightarrow W \otimes H + \varepsilon \qquad (6)$$

whereby a N (in this case N =2) dimensional matrix is decomposed into a series of positive shape functions (the columns of W and H) that when recombined using the kronecker product $\otimes$ and summed with an error matrix ε completely reconstitute the matrix W. As the dominant process was expected to be a two state unfolding N$\rightarrow$U a single non-negative factor was fitted

for all Hα chemical shifts for all measured residues for each denaturant separately, while excluding data from residues 1 and 20 due to 'end effects'. The resulting fits show very strong correlation between the two global fits of the folding curves (the first factor) and the measured data as shown in fig. 7, with only small residuals being observed.

Overall, on the time-scales measured and with the accuracy available from chemical shift data it can be concluded that the transition from N→U is highly consistent with a two-state process and no clear signs of intermediates species are detected even when examined on a per residue basis.

Molecular Dynamics Simulations

The principal purpose of running very long (microsecond) simulations at ambient temperature originating from the native structure of Trp-cage was to follow the unfolding dynamics in 2 M urea and GdmCl and compare them to the situation in neat water. The particular choice of 2 M solutions is advantageous in the sense that one can already see an effect of the denaturant on the miniprotein unfolding dynamics, nevertheless, the balance is not yet completely tilted toward unfolded structures. We extracted from the simulations several global coordinates (collective modes) of Trp-cage such as its root mean square deviation (RMSD) from the initial structure, the radius of gyration R_g, as well as parameters characterizing its helicity and compactness of the hydrophobic core, as defined below. In earlier studies, it has been proven useful to follow the time evolution of not just a single coordinate, but to correlate a pair of them.[26,39] Therefore, we adopt a similar approach to the analysis here, too, taking

advantage of the fact, that having a long MD trajectory allows us, unlike in REMD, to follow directly the dynamical evolution of the structure of Trp-cage.

Figs. 8-10 show the structural evolution of Trp-cage during a microsecond dynamics started with the native geometry in neat water, 2 M urea, and 2 M GdmCl. The 2D plots show correlated graphs of RMSD and R_g for six selected cumulative times (0-50, 0-200, 0-400, 0-600, and 0-1000 ns) together with 1D projections on the RMSD and R_g axes. At the same time, the actual position at these graphs at a given time is denoted by a cross and the corresponding geometry of Trp-cage is plotted. From these results it can be seen that in neat water (fig. 8) the system only slowly explores regions outside the native structure, which has RMSD smaller than 1 Å and R_g slightly above 7 Å and is characterized by a well developed α-helix and hydrophobic core stabilized by a Pro12/Trp6/Pro18 stacking motif and an outer Arg16-Asp9 salt bridge. Eventually, as dynamics proceeds geometries with RMSD up to 5 Å and R_g up to 10 Å are explored within the first microsecond, nevertheless the native structure remains the most populated one. This is because after exploring partially unfolded geometries the system frequently returns to (or close to) the native structure.

The situation is quantitatively different in 2 M urea or GdmCl (Figs. 9-10). Here, the system more quickly and easily leaves the native geometry basin and explores a much broader phase space region in RMSD and R_g during the microsecond dynamics. In the presence of denaturants, the system still does refold occasionally, but these events are less frequent than in neat water. The RMSD/R_g correlated plots in 2 M urea and GdmCl are rather similar to each other and, at each given time, the deviations between the two are small. In both cases, similar basins of structures are explored. Upon leaving the basin corresponding to the native structure

a phase space region with RMSD up to ~6 Å and R_g up to about 9 Å is dominantly explored. Within this region, two distinguishable basins develop in the course of the dynamics. The first one has roughly the same R_g as the native structure but an RMSD of 3 Å. Upon closer inspection this basin corresponds to folded structures with an almost intact α-helix but with a rearrangement in the hydrophobic core. Namely, a switch between two neighboring prolines in the meander part of the miniprotein occurred within the stabilizing Pro12/Trp6/Pro18 stacking motif.

In both denaturants the proline shift seems to be the first step in the unfolding process, which further leads to the second basin with R_g increased to 8 Å and RMSD of 3 Å. This basin cannot be represented by a single geometry but rather corresponds to a broader range of structures which contain both unfolded (or partially unfolded) helices and a destabilized hydrophobic core, in which the Arg16-Asp9 salt bridge is frequently destroyed. These structures are significantly more flexible and exposed to solvent that the native one or that of the first basin, being gateways to completely denatured geometries which have large values of both R_g and RMSD. These geometries, which are depicted in the upper right corner of the R_g/RMSD plots are explored both in urea and GdmCl solutions, with a somewhat larger occurrence in the former denaturant. The fact that the system spends a considerable time in this basin may to some extent be due to the employed force field, which is known to overestimate the unfolding temperature in neat water and in urea solutions.[3,39] Nevertheless, the proline shift is most likely a genuine part of the unfolding mechanism, although it may be of a more transient nature than observed in the present simulations.

Figs. 11-13 display the structural evolution of Trp-cage in terms of correlated plots of a helicity parameter characterizing the α-helix and a parameter monitoring the compactness of the hydrophobic core in neat water, 2 M urea, and 2 M GdmCl. The helicity parameter is the RMSD from the native structure, evaluated only for backbone heavy atoms forming the α-helix, while the core parameter is the mean distance between the Trp6 residue and the three nearest amino acids forming the hydrophobic core - the two nearest Pro residues and Tyr3. The native structure is characterized by both a high helical content and the compactness of the core. In neat water, the explored phase space during the microsecond trajectory gradually broadens but the focal point remains the native structure (fig. 11). Only after 500 ns does a shallow secondary basin with the helix RMSD around 2 Å and the core parameter between 7 and 8 Å develop, which corresponds to unfolded structures. In 2 M urea (fig. 12) or GdmCl (fig. 13) a much broader region of phase space is explored during the 1000 ns simulation, including frequent appearances of structures with a complete loss of helicity and/or destroyed hydrophobic core. The difference between the effects of the two denaturants is not large, with the phase space of possible structures being explored somewhat faster and more extensively in 2 M urea than in 2 M GdmCl.

The present microsecond simulations represent the longest direct MD runs performed for Trp-cage so far. They are, however, not long enough to provide converged phase space distributions of structures, unlike the recent REMD simulations.[3,39] The goal of the present work has been different - to follow for a sufficiently long time the unfolding dynamics of Trp-cage in neat water and in the presence of denaturants, so that the dynamical details of the process could be unraveled. The statement that the present simulations are long enough to reach

meaningful conclusions is supported by the fact that during the microsecond runs we observe numerous transitions between the individual structural basins of the miniprotein characterized above. We even see that the (partially) unfolded structure refolds back to the native one before unfolding again. In neat water, 10 such refolding transitions were observed, with this number being roughly halved in 2 M urea or GdmCl.

Figs. 14-15 show distributions of urea and guanidinium around the Trp-cage miniprotein for four representative structures extensively sampled during the simulations. These are the native geometry, a folded structure with switched prolines (Pro18 $\rightarrow$ Pro17) in the hydrophobic core, a partially unfolded geometry with a compromised helix and core (and a destroyed salt bridge), and a fully unfolded structure. Urea distribution (fig. 14) around the folded structures is rather even with the affinities for residues forming both the α-helix and the hydrophobic loop continuing with the meander. This is due to the fact that urea primarily tends to interact with the oxygens (and to a lesser extent also hydrogens) of the peptide bonds. Upon Trp-cage unfolding, urea remains distributed along the backbone. Note that the representation of the distribution of urea around the miniprotein is less faithful for unfolded than folded structures, since the former case comprises many different geometries which are hard to overlay on a single representative structure. The distribution of guanidinium around Trp-cage (fig. 15) is less even than that of urea. Gdm prefers to interact with negatively charged Asp9 forming the salt bridge, as well as to stack with aromatic sidechains such as Tyr3 (fig. 15). This stacking is particularly strong for the aromatic Trp6 residue once the side chain is liberated from the hydrophobic core upon denaturation. It is remarkable that the rather different interaction patterns of urea vs guanidinium with Trp-cage lead only to small variations in the unfolding

pathways caused by these two denaturants. For comparison, we have also preformed 700 ns unfolding simulations of Trp-cage in 2 M urea or GdmCl using the parm99SB force field,[67] which was shown recently to reproduce the experimental melting temperature of this miniprotein.[39] The results, presented in figs. S4 and S5 in the Supproting Information, are roughly comparable to those obtained with the parm99 force field (figs. 14-15) except that the unfolding dynamics due to the two denaturants is somewhat slower. As a consequence, the region of the phase space explored is smaller (figs. S4-S5), which is also partly due to a 30% shorter simulation time. Nevertheless, the proline shift discovered in the early stages of Trp-cage unfolding using parm99 and discused above is observed also in simulations using the parm99SB force field.

Conclusions

We performed an extensive study of denaturation of a model Trp-cage miniprotein by urea and guanidinium using a combination of experimental techniques – CD, DSC, and NMR, and MD simulations. These experiments all measure different physical effects resulting from denaturation, from gross thermodynamic changes (DSC), over global changes in the alpha helical content (CD), to per residue changes in electronic environment (NMR). DSC monitors sizable changes in calorimetric curves in the 10 – 120 °C temperature interval induced already by 0.05 M of denaturants. However, the interpretation is not straightforward, particularly in urea in which elevated temperatures induce chemical changes. CD shows a gradual effect of denaturants on unwinding of the α-helix, with guanidinium being about twice as efficient as urea, similarly as observed for other proteins previously.[68] NMR experiments, analyzing

unfolded and folded state of the peptide on a per residue basis during the unfolding of Trp-cage with urea and guanidine hydrochloride, do not detect any clear signs of intermediates species, which is in line with conclusions from previous NMR of the system without denaturants.[11] Taken together, all these experimental techniques point to a simple, two-state unfolding mechanism of Trp-cage in both denaturants.

Very long (microsecond) MD simulations provide direct hints to the molecular mechanisms of the destabilizing action of urea and guanidinium on the miniprotein at ambient conditions. Although the simulations are not long enough to yield a fully converged distribution of folded and unfolded geometries, they provide statistically significant information about the time-dependent unfolding process, which is consistent with previous REMD simulations in neat water and urea.[3,29,30] At a 2 M concentration a clear unfolding action of the denaturants is observed, in agreement with the above experiments. Despite the fact, that urea and guanidinium have different affinities to protein components (i.e., backbone and sidechains of varying polarity and charge) the observed unfolding mechanism for Trp-cage is strikingly similar. First, an exchange of two proline residues in the hydrophobic core occurs, which destabilizes it and then leads to a subsequent collapse of the hydrophobic loop and the α-helix of Trp-cage, resulting in complete unfolding. From the MD simulations we conclude that urea is a somewhat more efficient overall destabilizer of Trp-cage than guanidinium, although CD measurements show that for unwinding the α-helix the order of denaturants is reversed. The detailed unfolding processes observed in MD simulations happen at a rate which is too fast to be distinguished in the present experiments, which essentially detect only the folded and

unfolded ensembles with ms temporal resolution at best. Faster techniques, such as fluorescence correlation spectroscopy can provide a connecting link and indeed points to the details of the folding/unfolding mechanism,[40] as observed in the simulations. MD on one hand and CD, DSC, and NMR on the other hand thus provide a complementary but consistent picture of urea or guanidinium induced denaturation of the Trp-cage miniprotein.

In this study we have revealed a new paradox by use of full length unfolding trajectories from molecular dynamics simulations and experimental data. While guanidinium and urea are clearly very different chemical denaturants both in structure and action, they result in unfoldings of Trp-cage that are hard to distinguish at the level of individual folding pathways and experimental ensemble based averages. This introduces new and interesting questions which need to be addressed for a range of proteins, including a possible hypothesis that guanidinium and urea both act to initiate and carry out unfolding but may not necessarily determine the pathway taken to achieve unfolding.

Acknowledgment

We thank Steve Homans and Deepak Canchi for valuable discussions. Support from the Czech Science Foundation (grant 203/08/0114), the Czech Ministry of Education (grant LC 512) and the Academy of Sciences (Praemium Academie) is gratefully acknowledged. JH thanks the International Max Planck Research School for support. GT is supported by funding from the University of Leeds.

Figure captions:

Figure 1: CD spectrum of Trp-cage (0.1mg/ml) in phosphate buffer (pH=7; 20 mM) at 2 ^{o}C.

Figure 2: Dependence of helix fraction f_H (%) on temperature in phosphate buffer and for different concentration of used denatuting agents. Helix fraction f_H (%) was calculated from intensity of circular dichroism negative band at 222nm (at 2 ^{o}C) according literature.[44]

Figure 3: Dependence of helix fraction f_H (%) on concentration of denatuting agents (urea in black and GdmCl in red). Helix fraction f_H (%) was calculated from intensity of circular dichroism negative band at 222nm (at 2 ^{o}C) according literature.[44]

Figure 4: Thermal denaturations of Trp-cage peptide monitored by DSC at a concentration of 0.75 mg/ml in 20 mM sodium phosphate, pH 7.0, and in the presence of GdmCl. The heating rate during experiment was 1 °C/min. Buffer-buffer scans were substracted from calorimetric traces to get baseline corrections.

Figure 5: Representative ^{1}H-^{13}C HSQC spectra of folded (panel A, 0 M urea) and unfolded (panel B, 5 M urea) Trp-cage (pH 7.0, 280 K, 15mM sodium phosphate, 500 HMz) used in this study. Peaks are labelled by their attached carbon, no stereo-specific assignments were made. The peaks shown in grey were not assigned in this study.

Figure 6: Representative titration curves residues selected from the secondary structure elements in Trp-cage. Panel A positions of the selected residues on the secondary structure elements: red Tyr-3 helix 1, Purple Pro-12 helix 2, Blue pro19 sheet 1. Panel plots of 1H and 13C chemical shift changes for Ha-Ca correlations peaks for the selected peaks as titrated by urea.

Peaks positions are shown by the coloured circles (offset for clarity in crowded areas of the spectra) which match the colours of the contours. Peaks which originate from other residues are shown in grey and the start and the ends of the titration are indicated by the molar urea concentration (urea concentrations: light green 0.0 M, cyan 1.0 M, brown 2.0 M, pink 3.0 M, purple 4.0 M, and dark green 5.0 M). Panel C correlations between ^{13}C and ^{1}H chemical shifts for Trp-cage denatured with urea (left column) and guanidinium (right column) at the selected residues. Points are labelled by the molar concentration of denaturant and where they appear in panel B are color coded in the same colors. Correlation coefficients for a linear fit of ^{13}C against ^{1}H chemical shifts are shown on each plot.

Figure 7: Panel A: mean and standard deviations of the correlation coefficient R for linear fitting of a set of ^{1}H shifts against denaturant to all other ^{1}H shifts measurements against denaturant excluding residues 1 and 20 (data for residues 10, 11 and 18 were not measured). Left panel urea (0-5 M) and right panel guanidinium (0-4.5 M). Panel B: correlation between the amplitude weighted first non negative factor for ^{1}H shifts against denaturant, and the measured data. Left panel urea (0-5 M), right panel guanidinium (0-4.5 M).

Figure 8: Trp-cage dynamics in neat water. Snapshots of the miniprotein structure and cummulative RMSD/R_g plots are shown at 50, 200, 400, 600, 800, and 1000 ns.

Figure 9: Trp-cage dynamics in 2 M urea. Snapshots of the miniprotein structure and cummulative RMSD/R_g plots are shown at 50, 200, 400, 600, 800, and 1000 ns.

Figure 10: Trp-cage dynamics in 2 M GdmCl. Snapshots of the miniprotein structure and cummulative RMSD/R_g plots are shown at 50, 200, 400, 600, 800, and 1000 ns.

Figure 11: Core-helicity plots in neat water. Snapshots of the miniprotein, highlighting the α-helix and the hydrophobic core, and cummulative core/helix RMSD parameter plots are shown at 50, 200, 400, 600, 800, and 1000 ns.

Figure 12: Core-helicity plots in 2 M urea. Snapshots of the miniprotein, highlighting the α-helix and the hydrophobic core, and cummulative core/helix RMSD parameter plots are shown at 50, 200, 400, 600, 800, and 1000 ns.

Figure 13: Core-helicity plots in 2 M GdmCl. Snapshots of the miniprotein, highlighting the α-helix and the hydrophobic core, and cummulative core/helix RMSD parameter plots are shown at 50, 200, 400, 600, 800, and 1000 ns.

Figure 14: Distribution of urea (yellow) around Trp-cage for four representative structures – the native geometry, the folded structure with a proline switch in the hydrophobic core, and the partially and fully unfolded structures.

Figure 15: Distribution of guanidinium (green) around Trp-cage for four representative structures – the native geometry, the folded structure with a proline switch in the hydrophobic core, and the partially and fully unfolded structures.

Figure 1

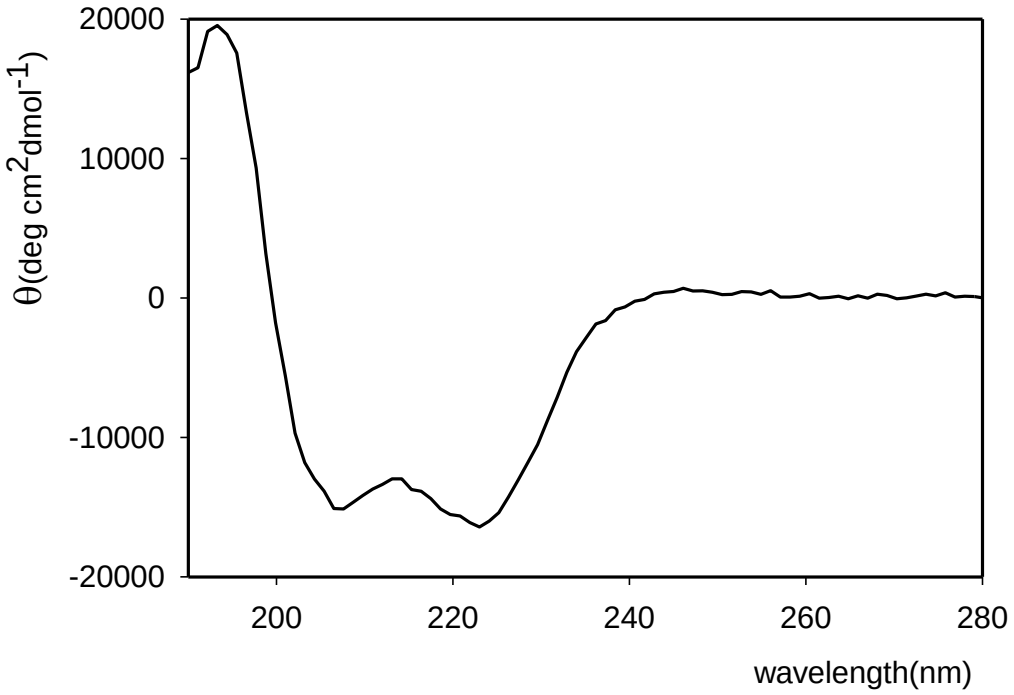
20000
10000
0
-10000
-20000
θ(deg cm2dmol-1)
200
220
240
260
280
wavelength(nm)

Figure 2

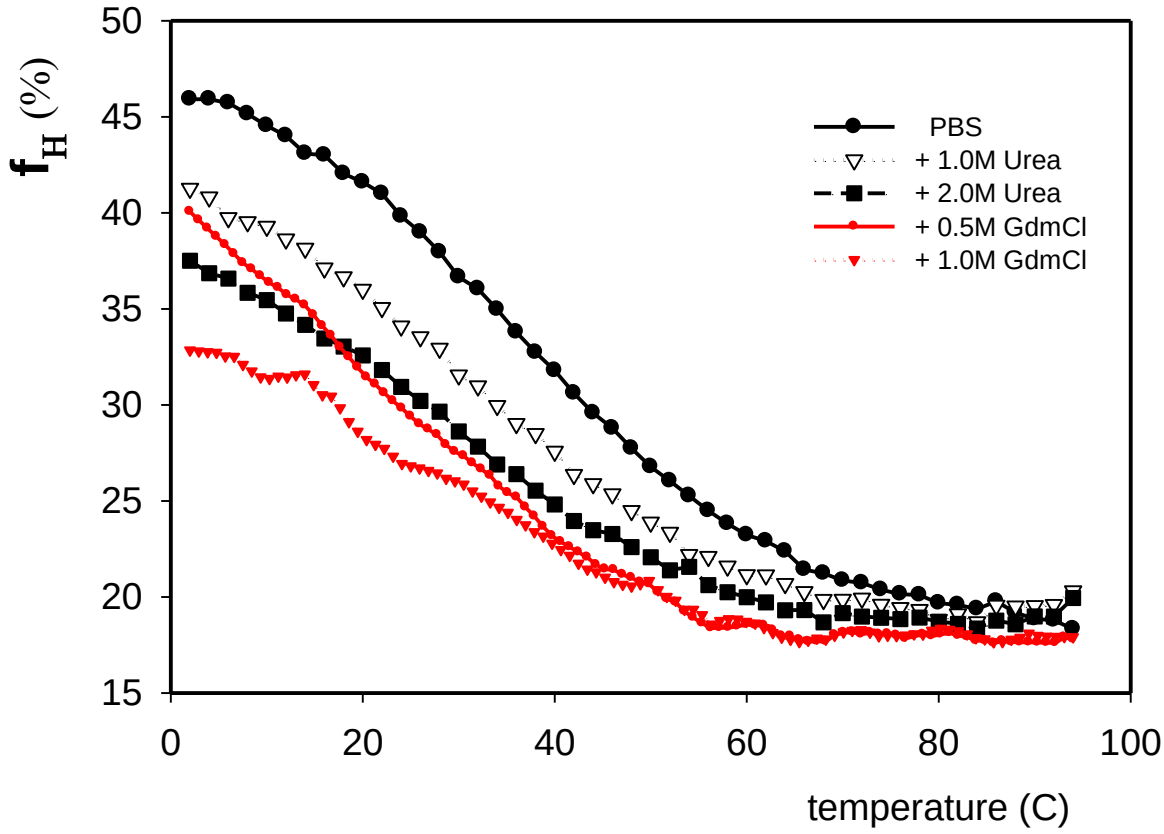
50
45
40
35
30
25
20
15
0
20
40
60
80
100
f_H (%)
temperature (C)
PBS
+ 1.0M Urea
+ 2.0M Urea
+ 0.5M GdmCl
+ 1.0M GdmCl

Figure 3

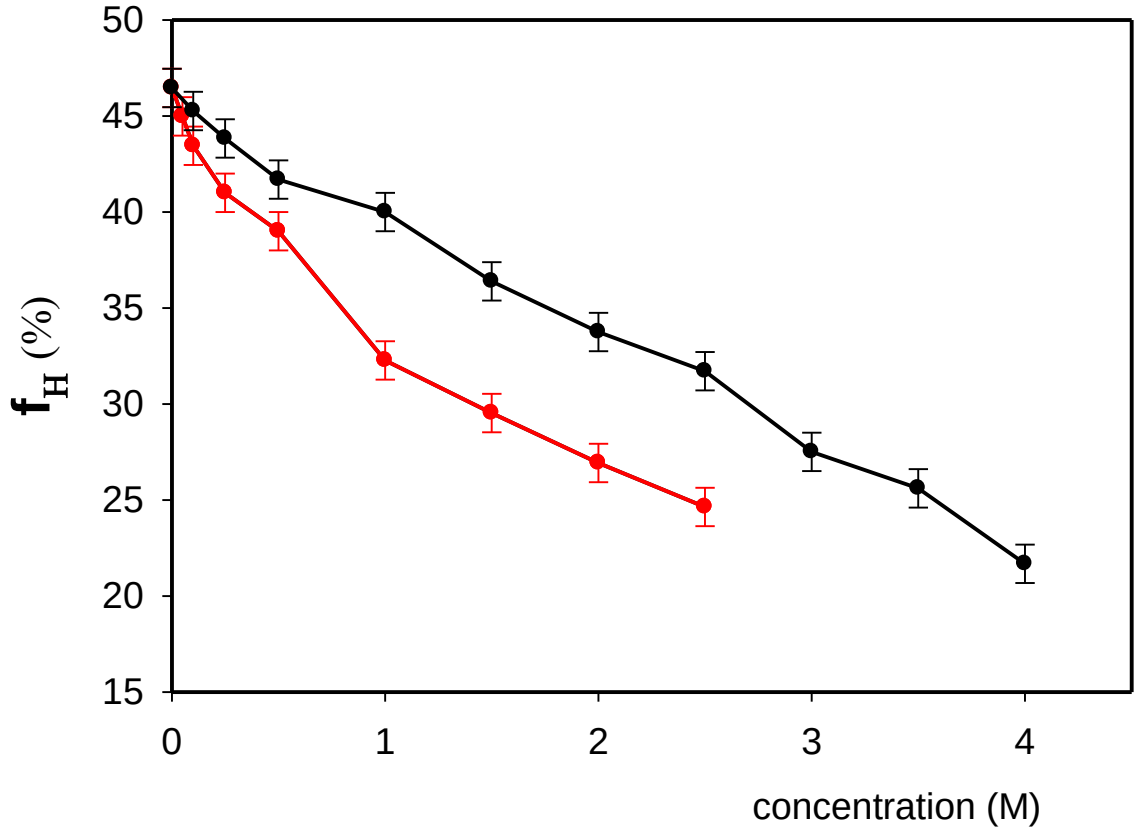

Figure 4

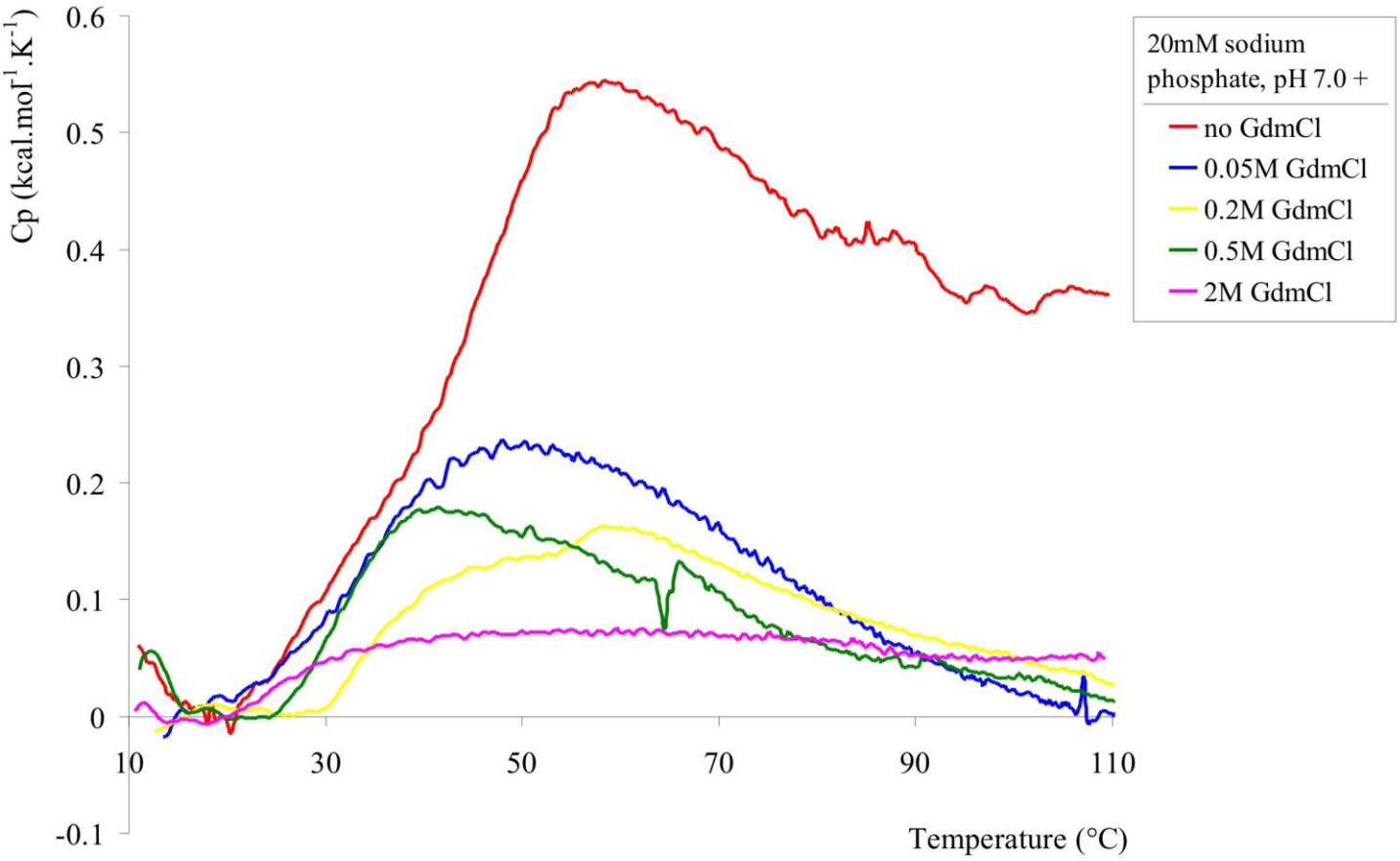
Cp (kcal.mol^{-1}.K^{-1})
0.6
0.5
0.4
0.3
0.2
0.1
0
-0.1
10
30
50
70
90
110
Temperature (°C)
20mM sodium phosphate, pH 7.0 +
no GdmCl
0.05M GdmCl
0.2M GdmCl
0.5M GdmCl
2M GdmCl

Figure 5

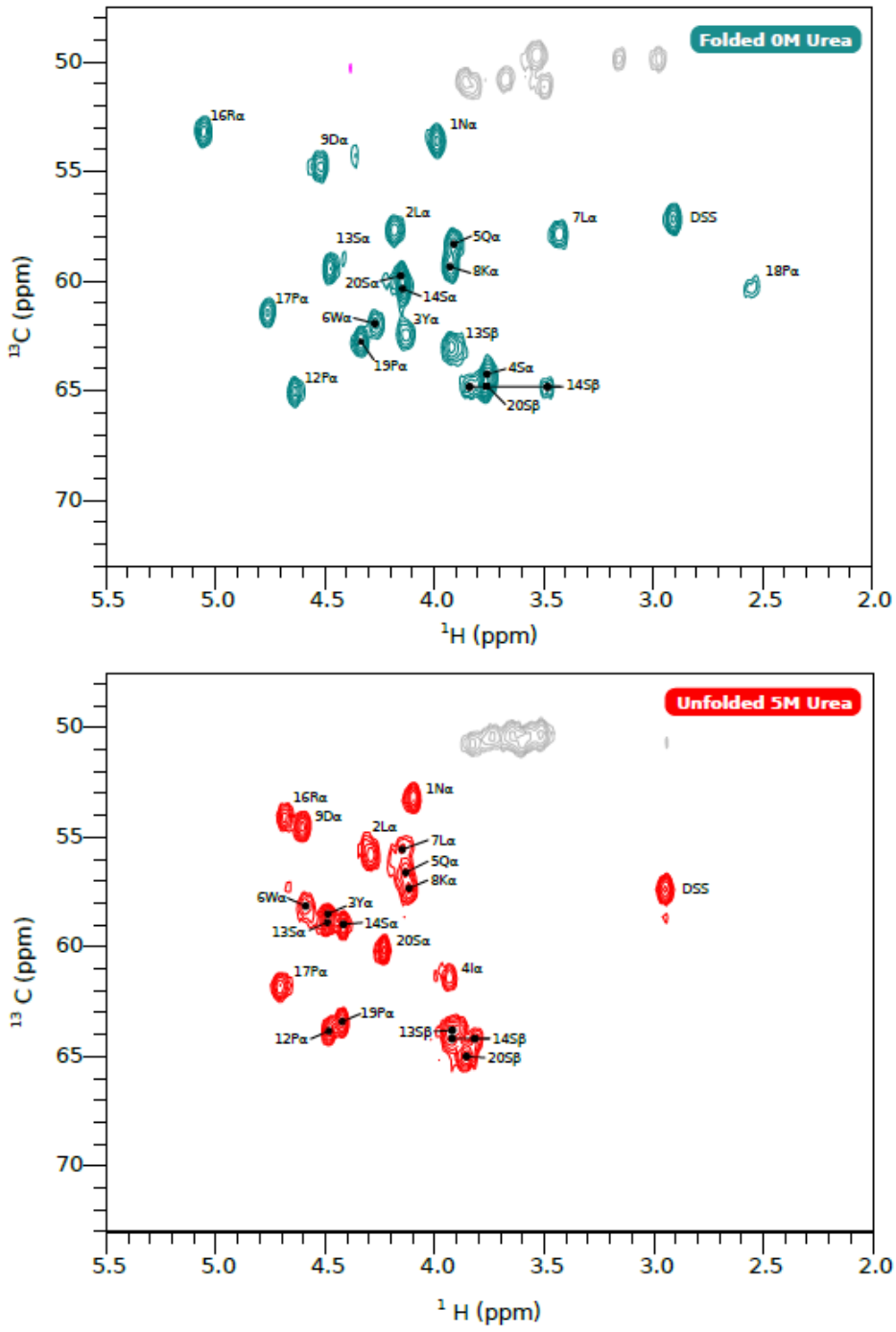
Folded 0M Urea
16Rα
9Dα
1Nα
2Lα
7Lα
DSS
13Sα
5Qα
8Kα
18Pα
20Sα
14Sα
17Pα
6Wα
3Yα
13Sβ
19Pα
4Sα
12Pα
14Sβ
20Sβ
^{13}C (ppm)
^{1}H (ppm)
Unfolded 5M Urea
16Rα
1Nα
9Dα
2Lα
7Lα
5Qα
8Kα
DSS
6Wα
3Yα
14Sα
13Sα
20Sα
4Iα
17Pα
19Pα
12Pα
13Sβ
14Sβ
20Sβ
^{13}C (ppm)
^{1}H (ppm)

Figure 6

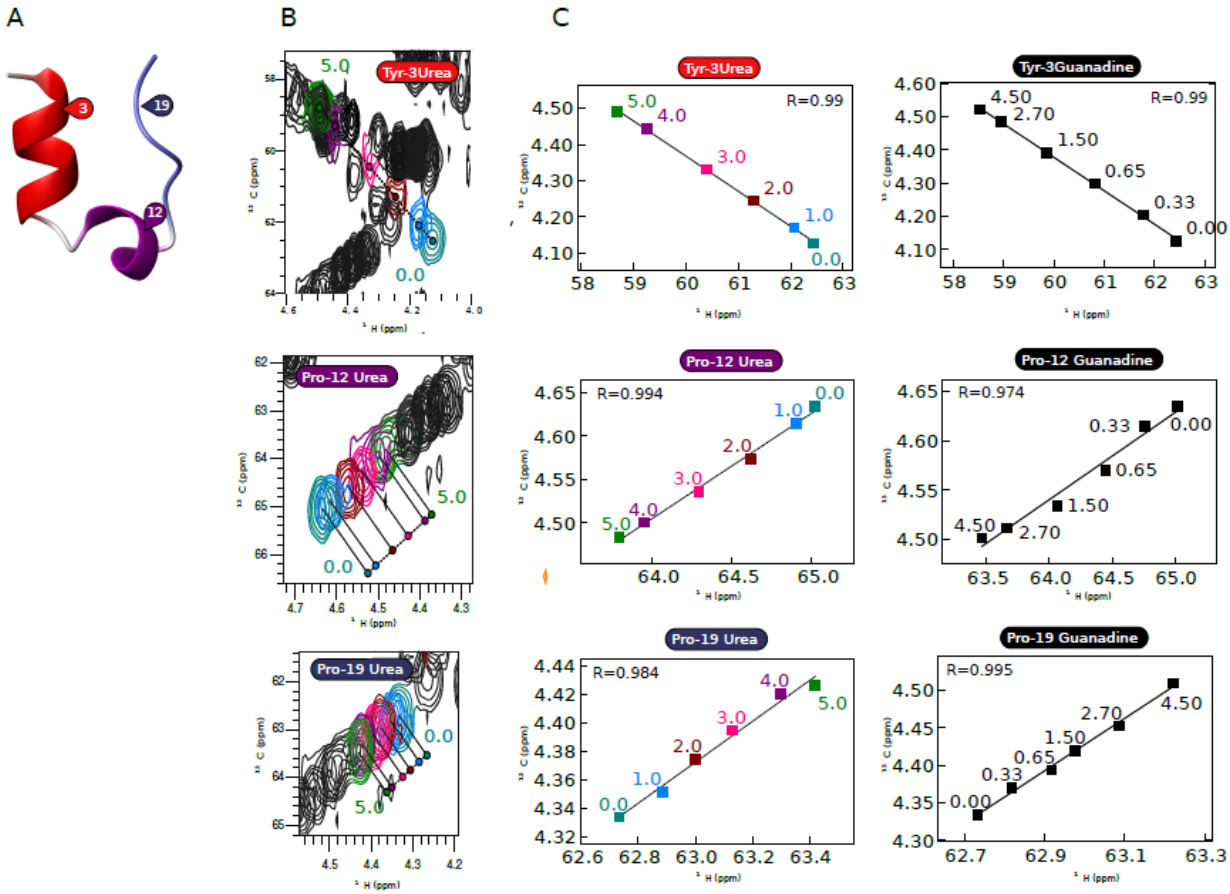
A
B
C
3
19
12
Tyr-3Urea
5.0
0.0
Pro-12 Urea
Pro-19 Urea
Tyr-3Guanadine
Pro-12 Guanadine
Pro-19 Guanadine
R=0.99
R=0.994
R=0.974
R=0.984
R=0.995
4.0
3.0
2.0
1.0
4.50
2.70
1.50
0.65
0.33
0.00

Figure 7

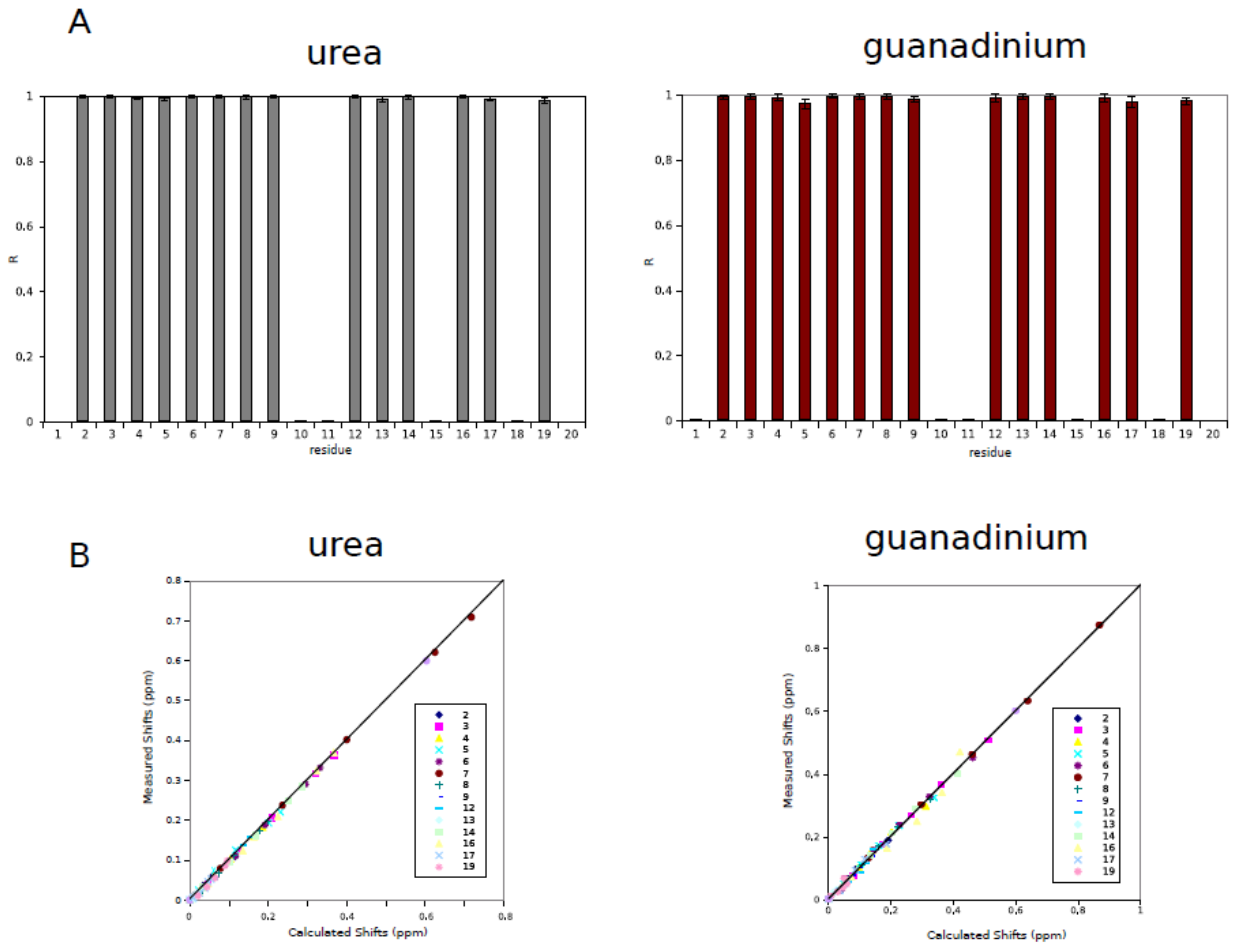
A
urea
guanadinium
R
residue
B
urea
guanadinium
Measured Shifts (ppm)
Calculated Shifts (ppm)

Figure 8

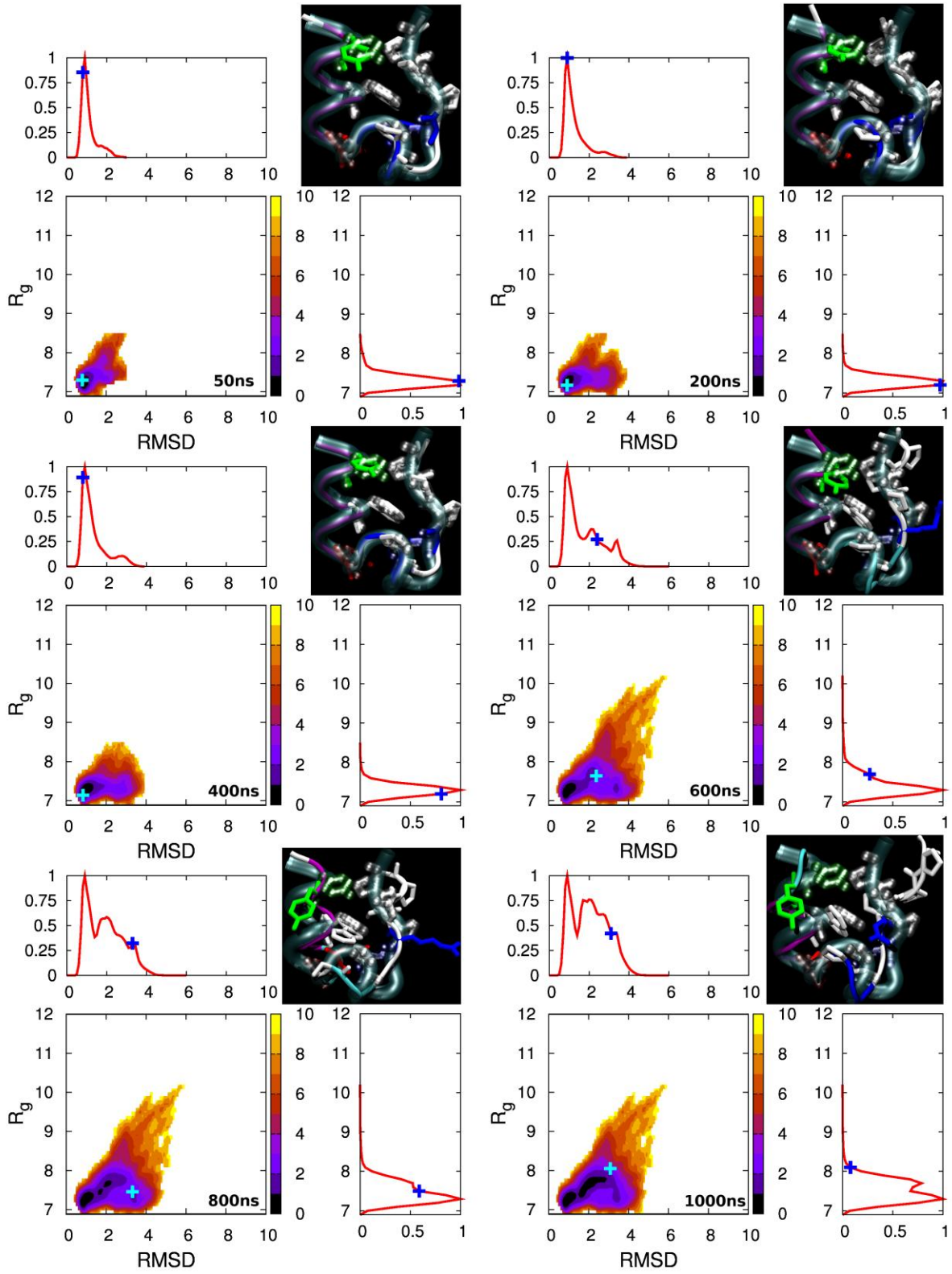

Figure 9

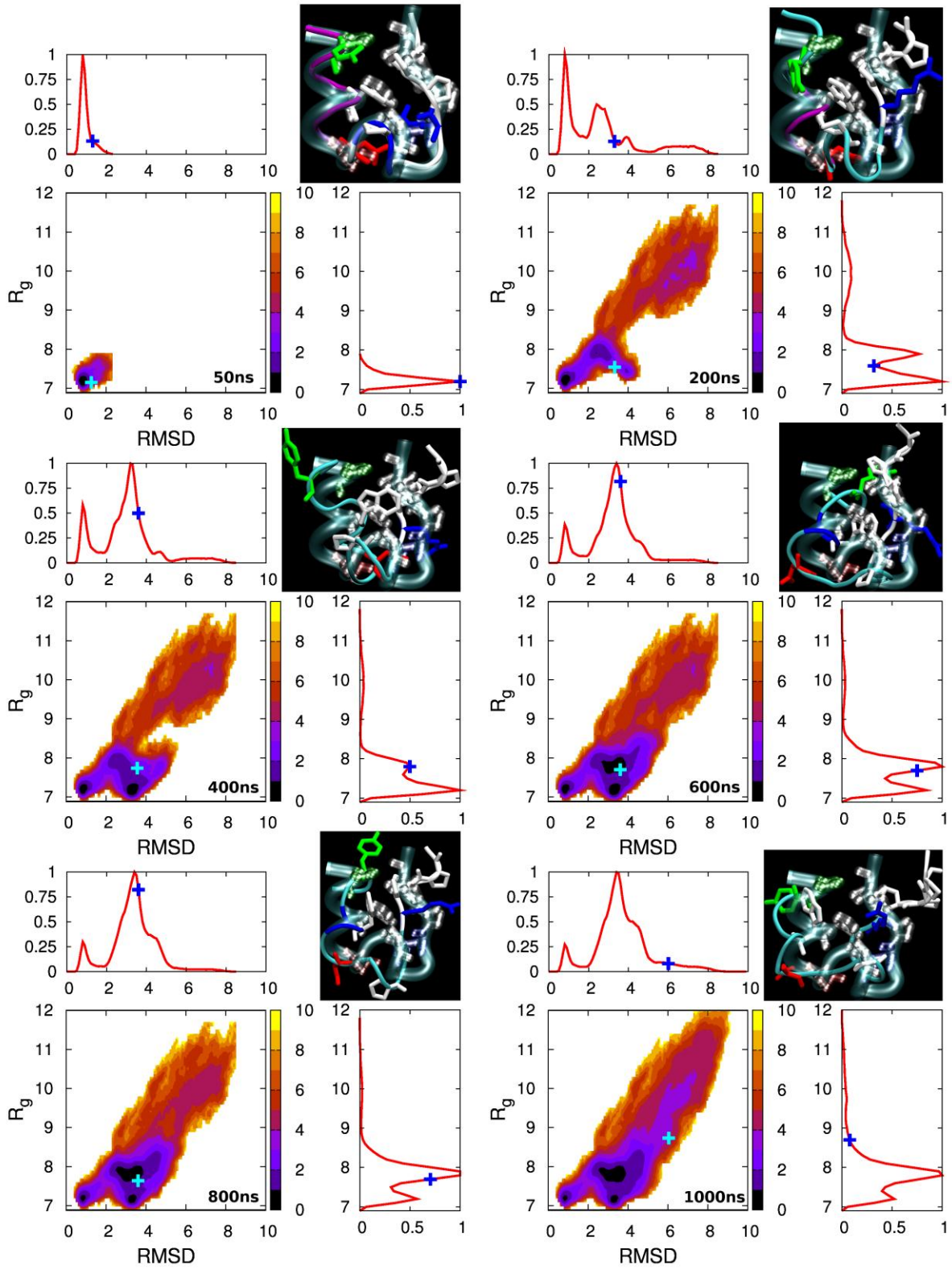

Figure 10

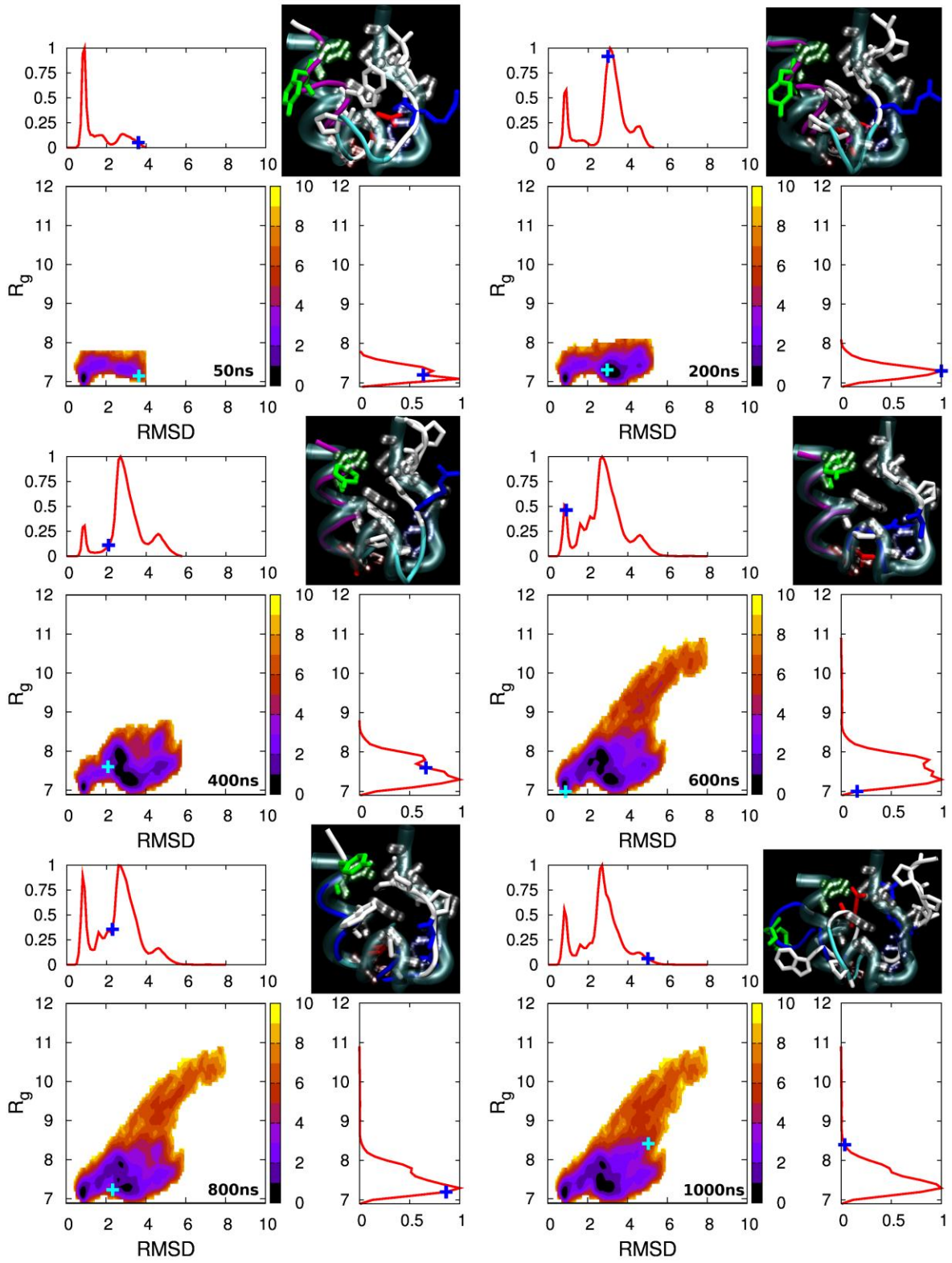

Figure 11

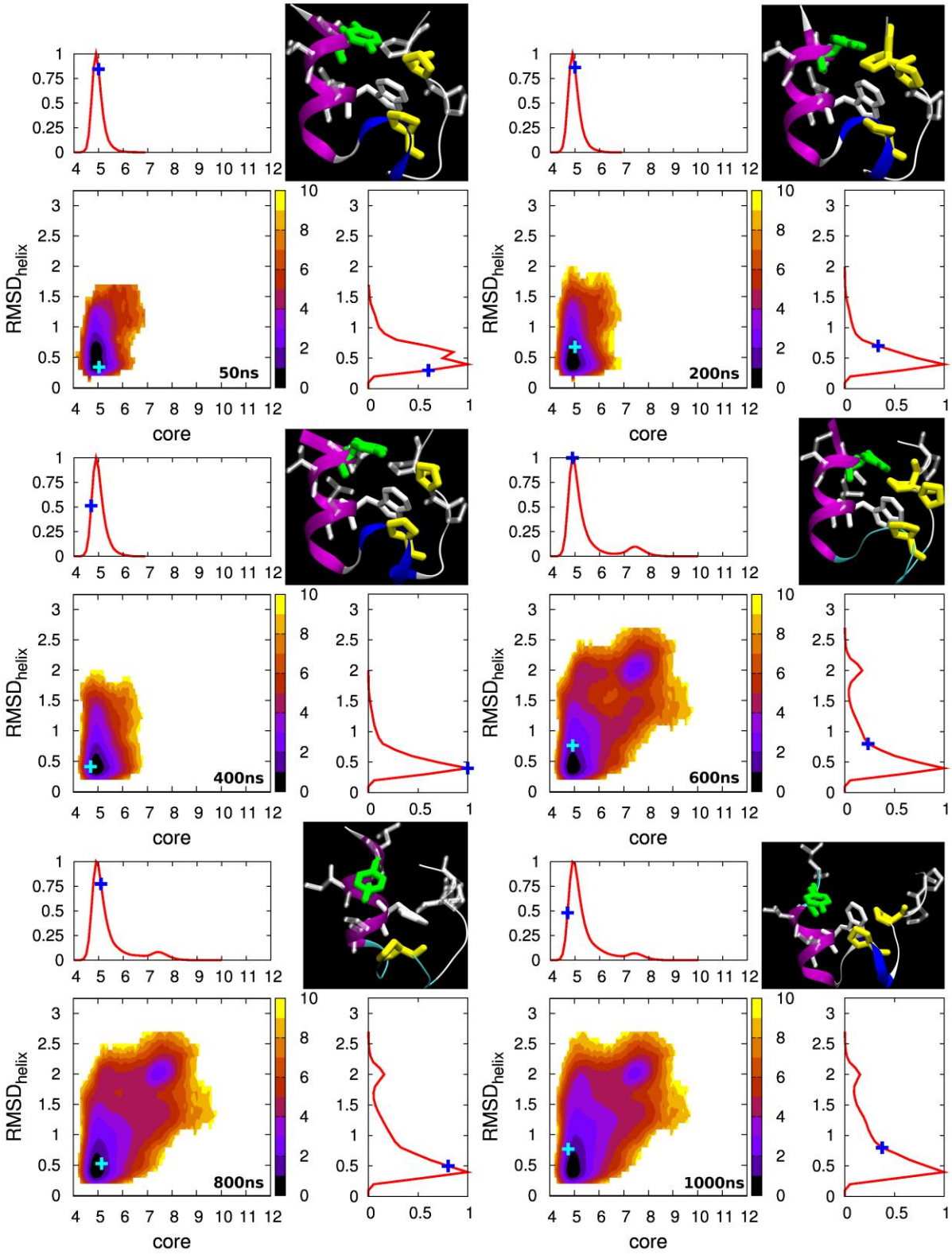

Figure 12

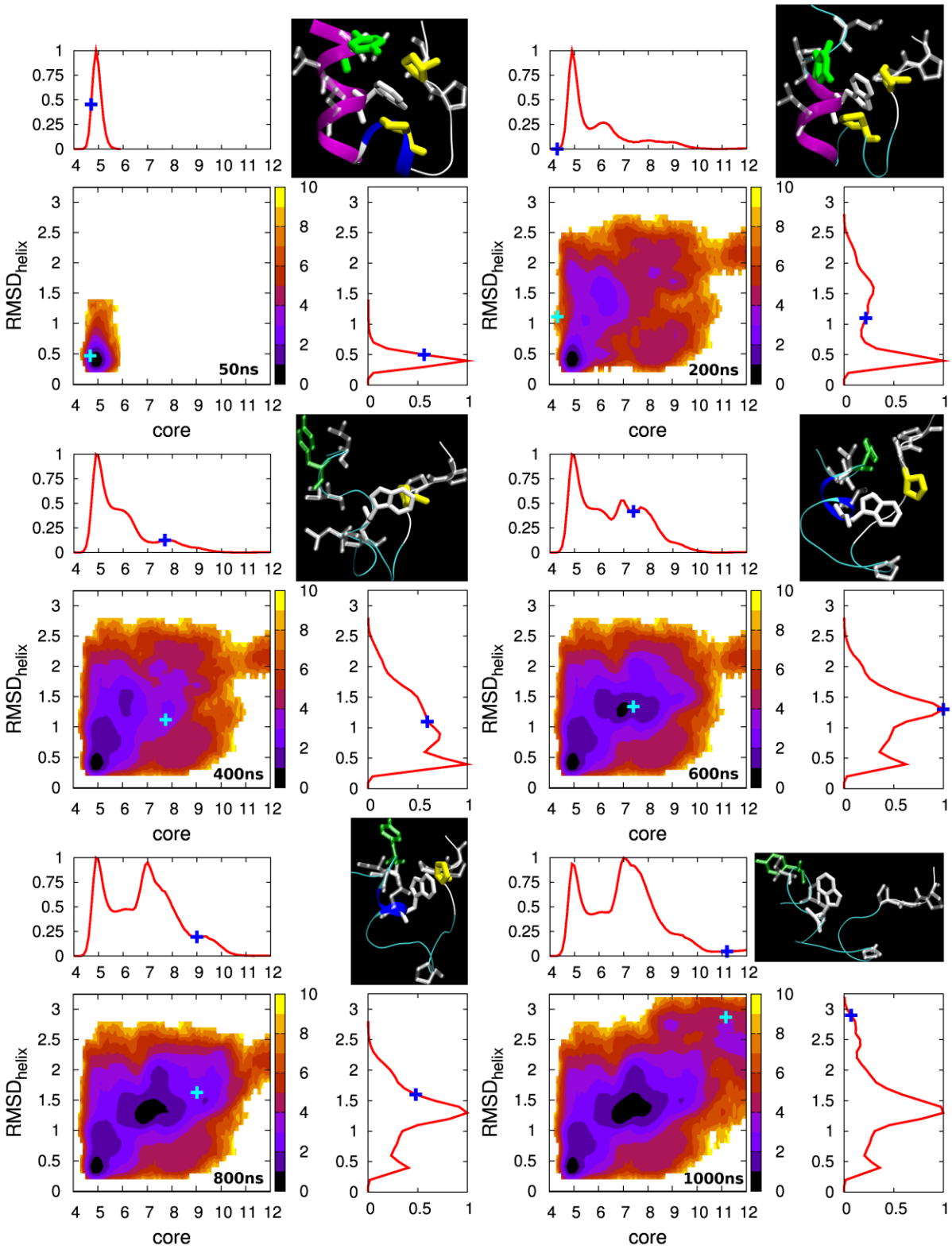

Figure 13

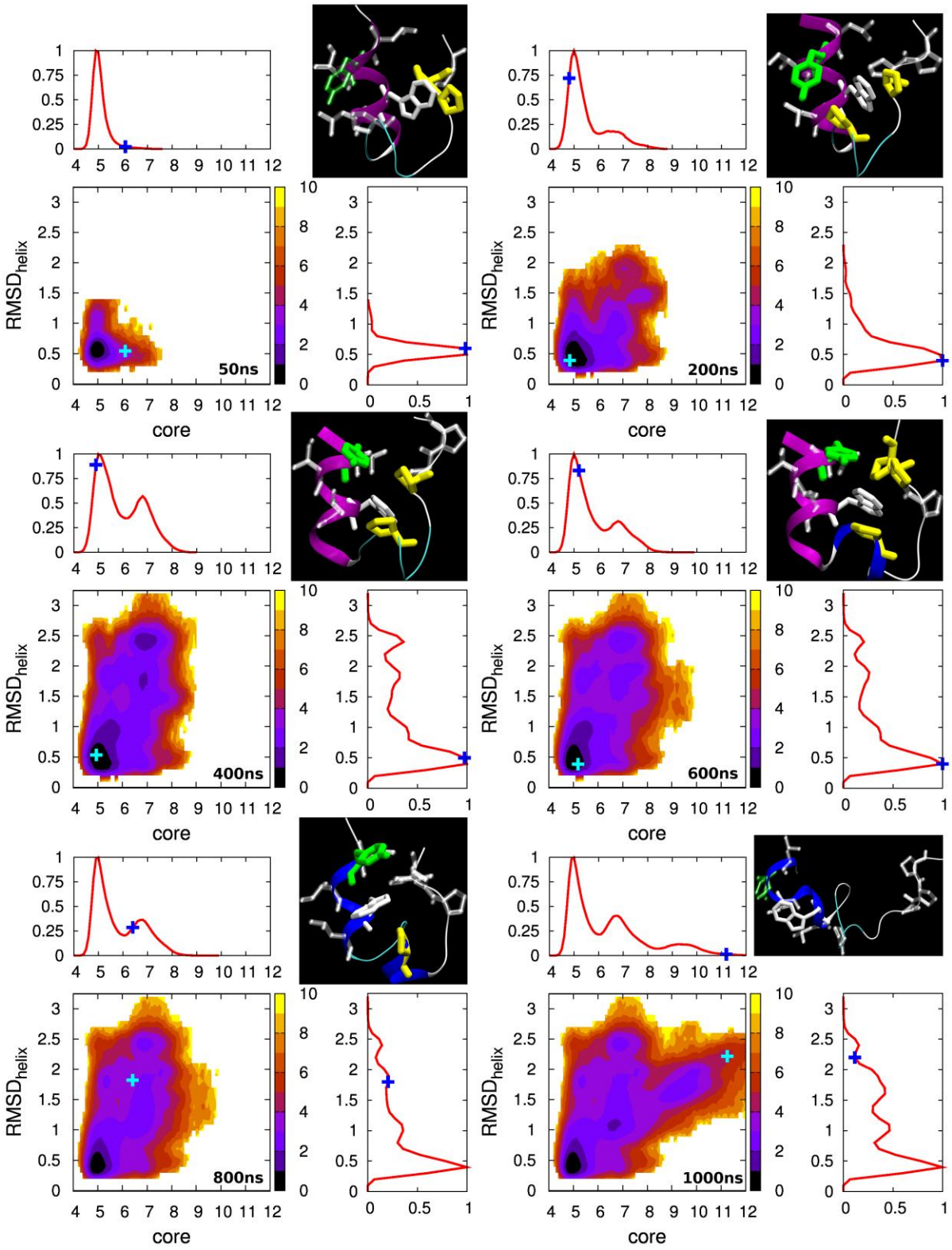

Figure 14

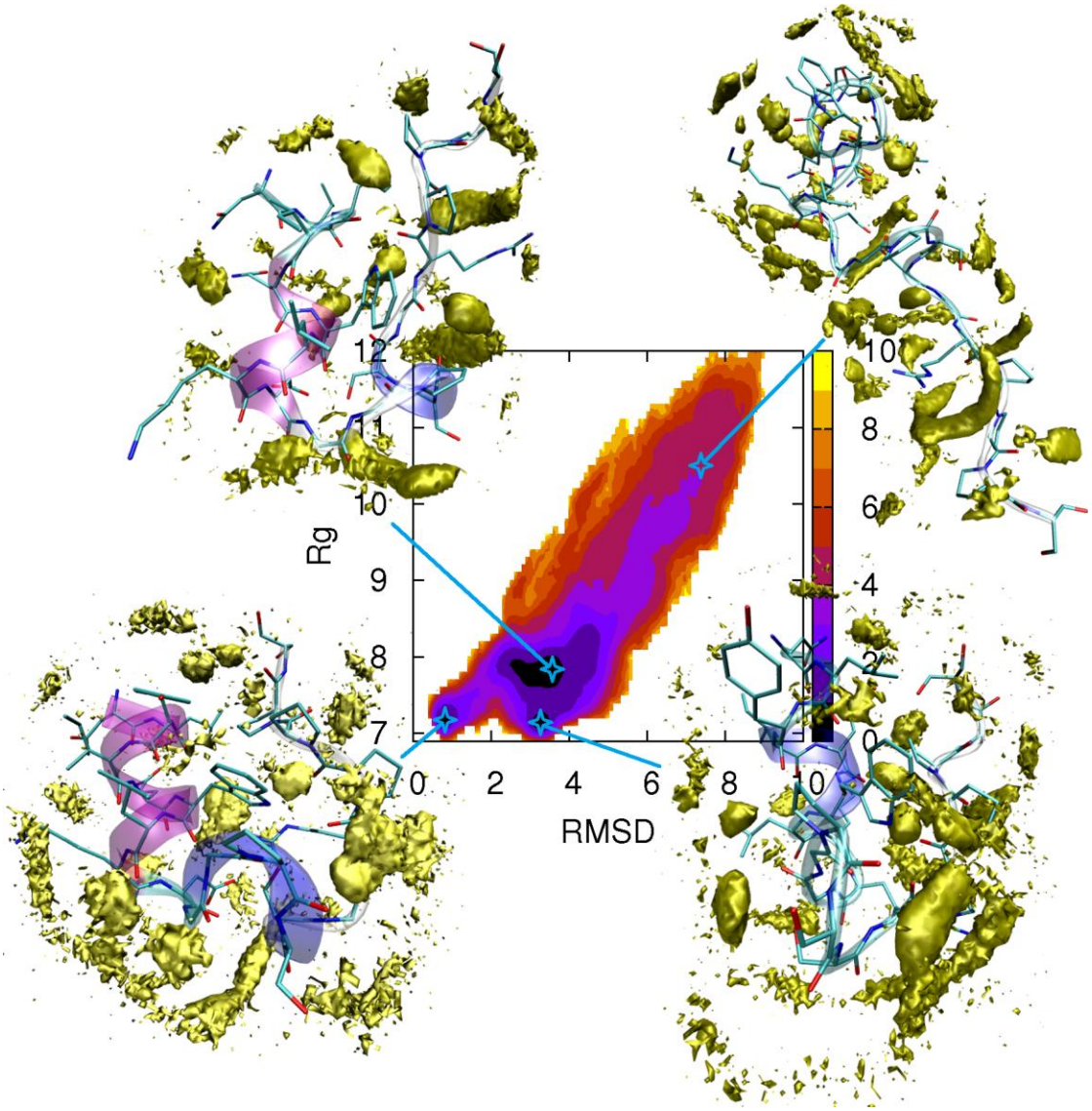

Figure 15

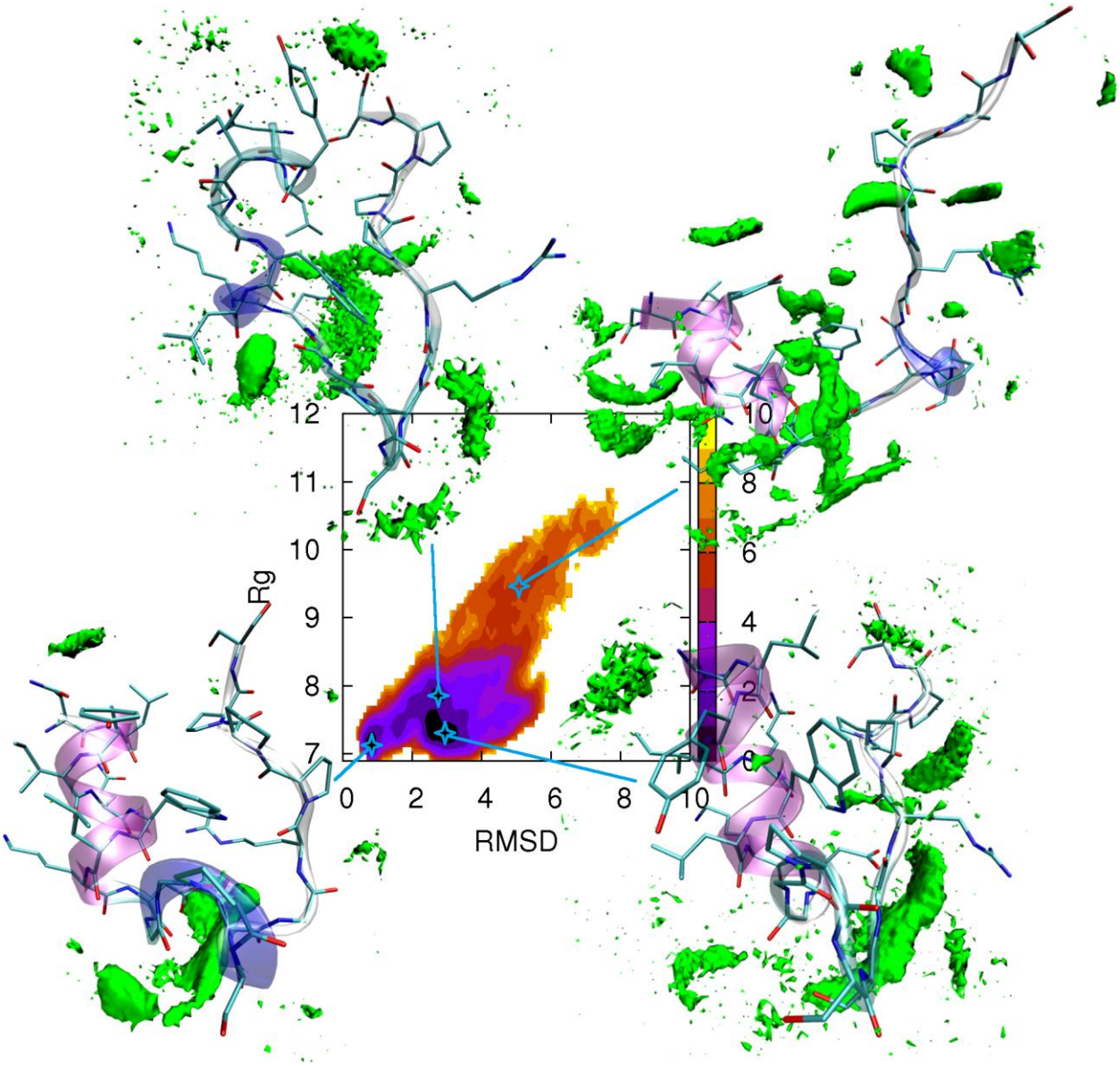

References

(1) Auton, M.; Holthauzen, L. M. F.; Bolen, D. W. *Proceedings of the National Academy of Sciences of the United States of America* **2007**, *104*, 15317-15322.

(2) Sagle, L. B.; Zhang, Y. J.; Litosh, V. A.; Chen, X.; Cho, Y.; Cremer, P. S. *Journal of the American Chemical Society* **2009**, *131*, 9304-9310.

(3) Canchi, D. R.; Paschek, D.; Garcia, A. E. *Journal of the American Chemical Society* **2010**, *132*, 2338-2344.

(4) Camilloni, C.; Rocco, A. G.; Eberini, I.; Gianazza, E.; Broglia, R. A.; Tiana, G. *Biophysical Journal* **2008**, *94*, 4654-4661.

(5) Stumpe, M. C.; Grubmuller, H. *Journal of the American Chemical Society* **2007**, *129*, 16126-16131.

(6) Mason, P. E.; Brady, J. W.; Neilson, G. W.; Dempsey, C. E. *Biophysical Journal* **2007**, *93*, L4-L6.

(7) O'Brien, E. P.; Dima, R. I.; Brooks, B.; Thirumalai, D. *Journal of the American Chemical Society* **2007**, *129*, 7346-7353.

(8) Lim, W. K.; Rosgen, J.; Englander, S. W. *Proceedings of the National Academy of Sciences of the United States of America* **2009**, *106*, 2595-2600.

(9) Das, A.; Mukhopadhyay, C. *Journal of Physical Chemistry B* **2009**, *113*, 12816-12824.

(10) Bolhuis, P. G. *Frontiers in Bioscience* **2009**, *14*, 2801-2828.

(11) Neidigh, J. W.; Fesinmeyer, R. M.; Andersen, N. H. *Nature Structural Biology* **2002**, *9*, 425-430.

(12) Gellman, S. H.; Woolfson, D. N. *Nature Structural Biology* **2002**, *9*, 408-410.

(13) Qiu, L. L.; Pabit, S. A.; Roitberg, A. E.; Hagen, S. J. *Journal of the American Chemical Society* **2002**, *124*, 12952-12953.

(14) Streicher, W. W.; Makhatadze, G. I. *Biochemistry* **2007**, *46*, 2876-2880.

(15) Adams, C. M.; Kjeldsen, F.; Patriksson, A.; van der Spoel, D.; Graslund, A.; Papadopoulos, E.; Zubarev, R. A. *International Journal of Mass Spectrometry* **2006**, *253*, 263-273.

(16) Copps, J.; Murphy, R. F.; Lovas, S. *Biopolymers* **2007**, *88*, 427-437.

(17) Hudaky, P.; Straner, P.; Farkas, V.; Varadi, G.; Toth, G.; Perczel, A. *Biochemistry* **2008**, *47*, 1007-1016.

(18) Iavarone, A. T.; Patriksson, A.; van der Spoel, D.; Parks, J. H. *Journal of the American Chemical Society* **2007**, *129*, 6726-6735.

(19) Mok, K. H.; Kuhn, L. T.; Goez, M.; Day, I. J.; Lin, J. C.; Andersen, N. H.; Hore, P. J. *Nature* **2007**, *447*, 106-109.

(20) Shi, X. G.; Parks, J. H. *Journal of the American Society for Mass Spectrometry* **2010**, *21*, 707-718.

(21) Wafer, L. N. R.; Streicher, W. W.; Makhatadze, G. I. *Proteins-Structure Function and Bioinformatics* **2010**, *78*, 1376-1381.

(22) Chowdhury, S.; Lee, M. C.; Xiong, G. M.; Duan, Y. *Journal of Molecular Biology* **2003**, *327*, 711-717.

(23) Linhananta, A.; Boer, J.; MacKay, I. *Journal of Chemical Physics* **2005**, *122*.

(24) Pitera, J. W.; Swope, W. *Proceedings of the National Academy of Sciences of the United States of America* **2003**, *100*, 7587-7592.

(25) Snow, C. D.; Zagrovic, B.; Pande, V. S. *Journal of the American Chemical Society* **2002**, *124*, 14548-14549.

(26) Zhou, R. H. *Proceedings of the National Academy of Sciences of the United States of America* **2003**, *100*, 13280-13285.

(27) Bunagan, M. R.; Yang, X.; Saven, J. G.; Gai, F. *Journal of Physical Chemistry B* **2006**, *110*, 3759-3763.

(28) Juraszek, J.; Bolhuis, P. G. *Proceedings of the National Academy of Sciences of the United States of America* **2006**, *103*, 15859-15864.

(29) Paschek, D.; Hempel, S.; Garcia, A. E. *Proceedings of the National Academy of Sciences of the United States of America* **2008**, *105*, 17754-17759.

(30) Paschek, D.; Nymeyer, H.; Garcia, A. E. *Journal of Structural Biology* **2007**, *157*, 524-533.

(31) Duan, L. L.; Mei, Y.; Li, Y. L.; Zhang, Q. G.; Zhang, D. W.; Zhang, J. Z. *Science China-Chemistry* **2010**, *53*, 196-201.

(32) Gattin, Z.; Riniker, S.; Hore, P. J.; Mok, K. H.; van Gunsteren, W. F. *Protein Science* **2009**, *18*, 2090-2099.

(33) Kannan, S.; Zacharias, M. *Proteins-Structure Function and Bioinformatics* **2009**, *76*, 448-460.

(34) Marinelli, F.; Pietrucci, F.; Laio, A.; Piana, S. *Plos Computational Biology* **2009**, *5*.

(35) Sarupria, S.; Ghosh, T.; Garcia, A. E.; Garde, S. *Proteins-Structure Function and Bioinformatics* **2010**, *78*, 1641-1651.

(36) Sugita, Y.; Okamoto, Y. *Chemical Physics Letters* **1999**, *314*, 141-151.

(37) Lee, M. S.; Olson, M. A. *Journal of Chemical Theory and Computation* **2010**, *6*, 2477-2487.

(38) Juraszek, J.; Bolhuis, P. G. *Biophysical Journal* **2008**, *95*, 4246-4257.

(39) Day, R.; Paschek, D.; Garcia, A. E. *Proteins-Structure Function and Bioinformatics* **2010**, *78*, 1889-1899.

(40) Neuweiler, H.; Doose, S.; Sauer, M. *Proceedings of the National Academy of Sciences of the United States of America* **2005**, *102*, 16650-16655.

(41) Smith, J. S.; Scholtz, J. M. *Biochemistry* **1996**, *35*, 7292-7297.

(42) Mason, P. E.; Dempsey, C. E.; Neilson, G. W.; Kline, S. R.; Brady, J. W. *Journal of the American Chemical Society* **2009**, *131*, 16689-16696.

(43) Vondrasek, J.; Mason, P. E.; Heyda, J.; Collins, K. D.; Jungwirth, P. *Journal of Physical Chemistry B* **2009**, *113*, 9041-9045.

(44) Rohl, C. A.; Baldwin, R. L. *Energetics of Biological Macromolecules, Part B* **1998**, *295*, 1-26.

(45) Piotto, M.; Saudek, V.; Sklenar, V. *Journal of Biomolecular Nmr* **1992**, *2*, 661-665.

(46) Kay, L. E.; Keifer, P.; Saarinen, T. *Journal of the American Chemical Society* **1992**, *114*, 10663-10665.

(47) Pace, C. N. In *Methods in Enzymology* 1986; Vol. 131, p 266.

(48) Delaglio, F.; Grzesiek, S.; Vuister, G. W.; Zhu, G.; Pfeifer, J.; Bax, A. *Journal of Biomolecular Nmr* **1995**, *6*, 277-293.

(49) Vranken, W. F.; Boucher, W.; Stevens, T. J.; Fogh, R. H.; Pajon, A.; Llinas, P.; Ulrich, E. L.; Markley, J. L.; Ionides, J.; Laue, E. D. *Proteins-Structure Function and Bioinformatics* **2005**, *59*, 687-696.

(50) Case, D. A. D., T. A.; Cheatham, III, T. E; Simmerling, C. L.; Wang, J.; Duke, R. E.; Luo, R.; Crowley, M.; Walker, R. C.; Zhang, W.; Merz, K. M.;Wang, B.; Hayik, S.; Roitberg, A.; Seabra, G.; Kolossvary, I.;Wong, K. F.; Paesani, F.; Vanicek, J.;Wu, X.; Brozell, S. R.; Steinbrecher, T.; Gohlke, H.; Yang, L.; Tan, C.; Mongan, J.; Hornak, V.; Cui, G.; Mathews, D. H.; Seetin, M. G.; Sagui, C.; Babin, V.; Kollman, P. A.; Amber 10, University of California, San Francisco: San Francisco, 2008.

(51) Berendsen, H. J. C.; Grigera, J. R.; Straatsma, T. P. *Journal of Physical Chemistry* **1987**, *91*, 6269-6271.

(52) Dang, L. X.; Chang, T. M. *Journal of Physical Chemistry B* **2002**, *106*, 235-238.

(53) Mason, P. E.; Neilson, G. W.; Enderby, J. E.; Saboungi, M. L.; Dempsey, C. E.; MacKerell, A. D.; Brady, J. W. *Journal of the American Chemical Society* **2004**, *126*, 11462-11470.

(54) Wang, J. M.; Wolf, R. M.; Caldwell, J. W.; Kollman, P. A.; Case, D. A. *Journal of Computational Chemistry* **2004**, *25*, 1157-1174.

(55) Cornell, W. D.; Cieplak, P.; Bayly, C. I.; Gould, I. R.; Merz, K. M.; Ferguson, D. M.; Spellmeyer, D. C.; Fox, T.; Caldwell, J. W.; Kollman, P. A. *Journal of the American Chemical Society* **1995**, *117*, 5179-5197.

(56) Weerasinghe, S.; Smith, P. E. *Journal of Physical Chemistry B* **2003**, *107*, 3891-3898.

(57) Essmann, U.; Perera, L.; Berkowitz, M. L.; Darden, T.; Lee, H.; Pedersen, L. G. *Journal of Chemical Physics* **1995**, *103*, 8577-8593.

(58) Berendsen, H. J. C.; Postma, J. P. M.; Vangunsteren, W. F.; Dinola, A.; Haak, J. R. *Journal of Chemical Physics* **1984**, *81*, 3684-3690.

(59) Ryckaert, J. P.; Ciccotti, G.; Berendsen, H. J. C. *Journal of Computational Physics* **1977**, *23*, 327-341.

(60) Rohl, C. A.; Baldwin, R. L. *Biochemistry* **1997**, *36*, 8435-8442.

(61) Rohl, C. A.; Baldwin, R. L. *Energetics of Biological Macromolecules*, 1998; Vol. 295.

(62) Wafer, L. N. R.; Streicher, W. W.; Makhatadze, G. I. *Proteins-Structure Function and Bioinformatics*, *78*, 1376-1381.

(63) Stark, G. R.; Stein, W. H. *Journal of Biological Chemistry* **1964**, *239*, 3755-&.

(64) Lippincott, J.; Apostol, I. *Analytical Biochemistry* **1999**, *267*, 57-64.

(65) Makhatadze, G. I.; Privalov, P. L. *Journal of Molecular Biology* **1992**, *226*, 491-505.

(66) Lee, D. D.; Seung, H. S. In *Advances in Neural Information Processing Systems 13*; Leen, T. K., Dietterich, T. G., Tresp, V., Eds. 2001; Vol. 13, p 556-562.

(67) Hornak, V.; Abel, R.; Okur, A.; Strockbine, B.; Roitberg, A.; Simmerling, C. *Proteins-Structure Function and Bioinformatics* **2006**, *65*, 712-725.

(68) Makhatadze, G. I. *Journal of Physical Chemistry B* **1999**, *103*, 4781-4785.